Acta Mathematica Scientia, 2020, **40B**(2): 572–588
https://doi.org/10.1007/s10473-020-0218-2

Acta Mathematica Scientia 数学物理学报
http://actams.wipm.ac.cn

EXPANDABLE PARALLEL FINITE ELEMENT METHODS FOR LINEAR ELLIPTIC PROBLEMS*

Guangzhi DU (杜光芝)
School of Mathematics and Statistics, Shandong Normal University, Jinan 250014, China
E-mail: *guangzhidu@gmail.com*

Abstract In this article, two kinds of expandable parallel finite element methods, based on two-grid discretizations, are given to solve the linear elliptic problems. Compared with the classical local and parallel finite element methods, there are two attractive features of the methods shown in this article: 1) a partition of unity is used to generate a series of local and independent subproblems to guarantee the final approximation globally continuous; 2) the computational domain of each local subproblem is contained in a ball with radius of $O(H)$ (H is the coarse mesh parameter), which means methods in this article are more suitable for parallel computing in a large parallel computer system. Some a priori error estimation are obtained and optimal error bounds in both H^1-normal and L^2-normal are derived. Finally, numerical results are reported to test and verify the feasibility and validity of our methods.

Key words Two-grid method; expandable method; partition of unity; parallel algorithm; finite element method

2010 MR Subject Classification 65N15; 65N30; 65N55

1 Introduction

In recent years, the development of efficient parallel computing for PDEs with high resolution has been an hot research topic. On the basis of the understanding of the local and global properties of a finite element solution to PDEs with high resolution, a new local and parallel approach [20, 21], was first proposed for a class of linear and nonlinear elliptic boundary value problems by Xu and Zhou. This local and parallel finite element algorithm was further applied for the Stokes and Navier-Stokes equations by He et al. [12–14, 18] and for the mixed Stokes-Darcy problems by Du et al. [7–9]. The algorithm has low communication complexity and allows existing sequential existing codes to run in a parallel environment with little investment in recoding.

However, one disadvantage of these local finite element algorithms is that the finite element solution is in general discontinuous. To overcome this defect, the author in [20] modified the above method to ensure that the final approximation is continuous. Furthermore, some local finite element methods based on a partition of unity are proposed in [6, 15, 22–25] to derive the globally continuous solution by assembling all the local solutions via the flexible and controllable

*Received Februray 27, 2019; revised June 18, 2019. Subsidized by NSFC (11701343) and partially supported by NSFC (11571274, 11401466).

partition of unity functions. The partition of unity method [3, 17] introduces us to a flexible and controllable way to implement domain decomposition and construct a global solution. There are many interesting works about the partition of unity method. For example, Hou et al. [15] developed an expandable local and parallel two-grid finite element scheme by considering the case of the Poisson equation, while for the computational fluid dynamic problems, Zheng et al. [22–25] proposed some new partition of unity methods based on two-grid discretiaztions and Appelhans et al. [2] proposed a new, low-communication algorithm for solving PDEs on massively parallel computers based on range decomposition. Larson et al. [16] and Song et al. [19] utilized the partition of unity method as the localization technique in post-processing procedure, and Bank et al. [4] presented a new domain decomposition algorithm for the parallel finite element solution of elliptic partial differential equations.

Although the partition of unity method could derive the globally continuous solution, the error estimates heavily depend on the usage of the superapproximation property of finite element spaces. As we known, the usage of this property causes the embarrassed problem that the distance between the boundaries of a specific subdomain and its expansion should be of constant order. Therefore the expansion of the subdomain could not be arbitrary small even when the diameter of the subdomain tends to zero. This will lead to a vast waste of parallel computing resources. In [15], we proposed an expandable local and parallel two-grid finite element scheme to overcome the dependence on superapproximation. The scale of each subproblem can be arbitrary small as H tends to zero and every two adjacent subproblems only have a small overlapping. Superposition principle is used to generate a series of local and independent subproblems and to make the global approximation continuous. In order to obtain an approximation with same accuracy as the fine mesh standard Galerkin approximation, a few iterations ($O(|\ln H|^2)$ in 2-D or $O(|\ln H|)$ in 3-D respectively) are essential.

Following the idea in [15], two expandable two-grid parallel finite element methods are given to solve the linear elliptic problems. The first algorithm is one iterative form while the second method is one non-iterative form. As in [15], in order to derive optimal estimates, a few iterations ($O(|\ln H|^2)$ in 2-D or $O(|\ln H|)$ in 3-D) are essential for the iterative method. However, for the non-iterative form, patches of diameter $O(|\ln H|^2)H$ or $O(|\ln H|)H$ in 2-D or 3-D respectively are sufficient to guarantee the same accuracy as the fine mesh standard Galerkin approximation because errors decay exponentially with respect to the number of layers of elements in patches (see [11] for detail). Both the two algorithms can reach the same accuracy as the fine mesh standard Galerkin approximation in theoretical analysis and numerical simulation.

From the visual point of view, the non-iterative form has a similar approach except patch is a m-layer. But in practice, the non-iterative form needs only one global communication to derive the globally continuous approximation, while for the iterative form, in each iteration, one global communication is essential to reach the global approximation. That is the non-iterative form needs less communication than the iterative form.

The outline of this article is organized as follows. In Section 2, some preliminary materials and assumptions on mixed finite element spaces are provided. In Section 3, two expandable two-grid parallel finite element methods are presented. In Section 4, some a priori error estimation and optimal error bounds in both H^1 and L^2-normal for the two algorithms are derived. In Section 5, some numerical experiments are reported to show the validity of our algorithms.

Finally, a short conclusion is given.

2 Preliminaries

In this article, we consider the following linear elliptic equations with Dirichlet boundary condition defined in convex bounded domain $\Omega \subset R^d$, $d = 2, 3$:

$$\begin{cases} -\Delta u + \mathbf{b} \cdot \nabla u = f, & \text{in } \Omega, \\ u = 0, & \text{on } \partial\Omega. \end{cases} \tag{2.1}$$

For a nonnegative integer s, we denote by $H^s(\Omega)$ the Sobolev space [1] in usual sense and their associated norms $\|\cdot\|_{s,\Omega}$, while denote by $H_0^1(\Omega)$ the closed subspace of $H^1(\Omega)$ consisting of functions with zero trace on $\partial\Omega$. For convenience, the symbols $\lesssim$, $\gtrsim$ and $\cong$ will be used in this article. That $x_1 \lesssim y_1$, $x_2 \gtrsim y_2$, and $x_3 \cong y_3$ mean that $x_1 \leq C_1 y_1$, $x_2 \geq c_2 y_2$, and $c_3 x_3 \leq y_3 \leq C_3 x_3$ for some constants C_1, c_2, c_3, and C_3 independent of mesh size. For sub-domains $S_1 \subset S_2 \subset \Omega$, we write $S_1 \subset\subset S_2$ to mean that $\text{dist}(\partial S_2 \backslash \partial\Omega, \partial S_1 \backslash \partial\Omega) > 0$.

In the following, we denote by $(\cdot, \cdot)$ the L^2-inner product on Ω. Thus, $\|\cdot\|_{0,\Omega} = (\cdot, \cdot)^{\frac{1}{2}}$. Let us define $a(\cdot, \cdot)$ as $a(u, v) = (\nabla u, \nabla v) + (\mathbf{b} \cdot \nabla u, v)$, $\forall u, v \in H_0^1(\Omega)$, where $(\cdot, \cdot)$ is the standard inner-product of $L^2(\Omega)$. Then, the weak formulation of (2.1) reads: find $u \in H_0^1(\Omega)$ such that

$$a(u, v) = (f, v), \quad \forall v \in H_0^1(\Omega). \tag{2.2}$$

A sufficient and necessary condition for the well-posedness of (2.2) is that

$$\|w\|_{1,\Omega} \lesssim \sup_{\phi \in H_0^1(\Omega)} \frac{a(w, \phi)}{\|\phi\|_{1,\Omega}}, \sup_{\phi \in H_0^1(\Omega)} \frac{a(\phi, w)}{\|\phi\|_{1,\Omega}}, \quad \forall w \in H_0^1(\Omega). \tag{2.3}$$

The variational problem (2.2) has a unique solution (see, for ample, [5]). Assume that $a(u, v)$ is continuous, that is,

$$a(u, v) \lesssim \|u\|_{1,\Omega} \|v\|_{1,\Omega}, \quad \forall u, v \in H_0^1(\Omega), \tag{2.4}$$

and coercive, that is,

$$\exists\, \beta^* > 0 : \ a(v, v) \geq \beta^* \|\nabla v\|_{0,\Omega}^2, \quad \forall v \in H_0^1(\Omega). \tag{2.5}$$

For a given bounded domain $\Omega \subset R^d$, we assume that $T^H(\Omega) = \{\tau_\Omega^H\}$ is a regular triangulation of Ω. Here, $H = \max_{\tau_\Omega^H \in T^H(\Omega)} \{\text{diam}(\tau_\Omega^H)\}$ is the mesh parameter. Associated with the mesh $T^H(\Omega)$, let $S^H(\Omega) = \{v_H \in C^0(\Omega) : v_H|_{\tau_\Omega^H} \in P_{\tau_\Omega^H}^r, \ \forall \tau_\Omega^H \in T^H(\Omega)\}$ be a C^0-finite element space on Ω and $S_0^H(\Omega) = S^H(\Omega) \cap H_0^1(\Omega)$, where $r \geq 1$ is a positive integer, and $P_{\tau_\Omega^H}^r$ is the space of polynomials of degree not greater than r defined on τ_Ω^H.

For these finite element spaces and problem (2.1), we make the following assumptions.

A1 Interpolation. There is a finite element interpolation I_H defined on $S^H(\Omega)$ such that for any $w \in H^s(\tau_\Omega^H)$, $0 \leq m \leq s \leq r + 1$,

$$\|w - I_H w\|_{m,\Omega} \lesssim H^{s-m} \|w\|_{s,\Omega}.$$

A2 Inverse Inequality. For any $w \in S^H(\Omega)$,

$$\|w\|_{1,\Omega} \lesssim H^{-1} \|w\|_{0,\Omega}.$$

A3 Regularity. For any $f \in H^{r-1}(\Omega)$, the solution of

$$a(u, v) = (f, v), \quad \forall v \in H_0^1(\Omega),$$

and its associated formal adjoint problem

$$a(v, u) = (f, v), \quad \forall v \in H_0^1(\Omega),$$

satisfiy

$$\|u\|_{r+1,\Omega} \lesssim \|f\|_{r-1,\Omega}.$$

Then, the standard Galerkin equation for solving (2.2) reads: find $u_H \in S_0^H(\Omega)$ such that

$$a(u_H, v_H) = (f, v_H), \quad \forall v_H \in S_0^H(\Omega). \tag{2.6}$$

For the standard Galerkin approximation u_H, we have the following assumption:

$$\|u - u_H\|_{0,\Omega} + H\|u - u_H\|_{1,\Omega} \lesssim H^{r+1}, \tag{2.7}$$

which can be easily verified as long as $u \in H^{r+1}(\Omega)$.

3 Numerical Algorithms

Assume that $\{\phi_i\}_{i=1}^N$ is a partition of unity on Ω for given integer $N \geq 1$ such that $\Omega \subset \bigcup_{i=1}^N \text{supp } \phi_i$ and $\sum_{i=1}^N \phi_i \equiv 1$ on Ω. There are many ways to construct the applicable partition of unity. A simple choice of the partition of unity is the piecewise linear Lagrange basis functions associated with the coarse grid triangulation $T^H(\Omega)$, where N is the number of vertices of $T^H(\Omega)$ including the boundary vertices.

For each vertex x_i of the coarse grid, let $\omega_i^0 = \text{supp } \phi_i = D_i$. We call ω_i^0 the patch of layer 0 defined on the ith vertex. Then, we can define the patch of layer m ($m \geq 1$, an integer) based on vertex i recursively. That is

$$\omega_i^m = \bigcup_{x_j \in \omega_i^{m-1}} \omega_j^0,$$

and the vertices on the boundary are included. For a proper chosen m, we denote $\omega_i = \omega_i^m$; see Figure 1. For fine mesh parameter h, we introduce following fine mesh finite element spaces $S^h(\omega_i)$, $S_0^h(\omega_i)$ and $S^h(\Omega)$, $S_0^h(\Omega)$, which have the same definitions as $S^H(\Omega)$ and $S_0^H(\Omega)$ given in the previous section.

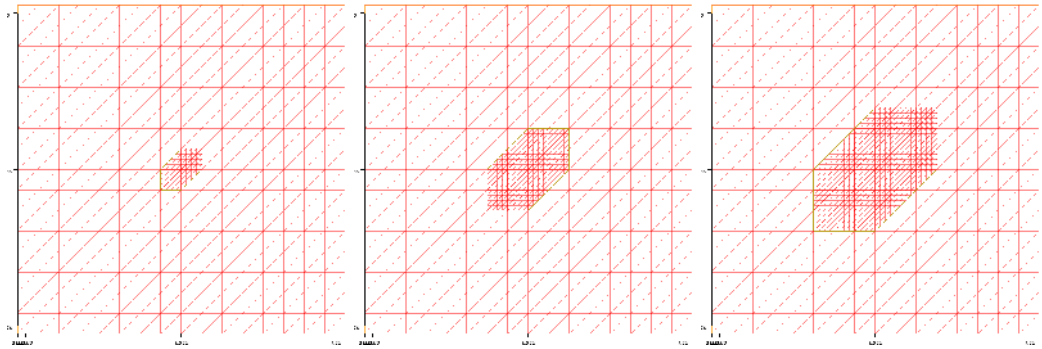

Figure 1 Patch of layer m ($m = 0, 1, 2$), from left to right

Algorithm 1 Iterative Form

1. Find a global coarse grid solution $u_H \in S_0^H(\Omega)$ such that

$$a(u_H, v_H) = (f, v_H), \quad \forall v_H \in S_0^H(\Omega). \tag{3.1}$$

2. Find local fine grid corrections $w_{H,h}^i \in S_0^h(\omega_i^1)$ such that

$$a(w_{H,h}^i, v) = (f, \phi_i v) - a(u_H, \phi_i v), \quad \forall v \in S_0^h(\omega_i^1),\ i = 1, 2, \cdots, N. \tag{3.2}$$

Set

$$w_{H,h} = \sum_{i=1}^{N} w_{H,h}^i, \quad u_{H,h} = u_H + w_{H,h}. \tag{3.3}$$

3. Do a global correction on the coarse gird: find $E_H \in S_0^H(\Omega)$ such that

$$a(E_H, v) = (f, v) - a(u_{H,h}, v), \quad \forall v \in S_0^H(\Omega). \tag{3.4}$$

And the final approximate solution is defined as

$$u_H^h = u_{H,h} + E_H. \tag{3.5}$$

In the later numerical tests, it is easy to find that errors of the expandable two-grid parallel finite element method decay exponentially with respect to the number of layers of elements in patches. Therefore, for a proper chosen m, which is relevant to coarse mesh size H, it is sufficient to guarantee the same accuracy as the fine mesh standard Galerkin approximation. Let us denote $\omega_i = \omega_i^m$, then we derive the following non-iterative form algorithm.

Algorithm 2 Non-iterative Form

1*. Find a global coarse grid solution $u_H \in S_0^H(\Omega)$ such that

$$a(u_H, v_H) = (f, v_H), \quad \forall v_H \in S_0^H(\Omega). \tag{3.6}$$

2*. Find local fine grid corrections $\hat{w}_{H,h}^i \in S_0^h(\omega_i)$ such that

$$a(\hat{w}_{H,h}^i, v) = (f, \phi_i v) - a(u_H, \phi_i v), \quad \forall v \in S_0^h(\omega_i),\ i = 1, 2, \cdots, N. \tag{3.7}$$

Set

$$\hat{u}_{H,h} = u_H + \sum_{i=1}^{N} \hat{w}_{H,h}^i. \tag{3.8}$$

3*. Do a global correction on the coarse gird: find $\hat{E}_H \in S_0^H(\Omega)$ such that

$$a(\hat{E}_H, v) = (f, v) - a(u_{H,h}, v), \quad \forall v \in S_0^H(\Omega). \tag{3.9}$$

And the final approximate solution is defined as

$$\hat{u}_H^h = \hat{u}_{H,h} + u_H. \tag{3.10}$$

Remark It is obvious that all the subproblems in Step 2 and 2* are independent, once the global coarse grid solution u_H is known and the scale of each subproblem in Step 2 and 2* can be arbitrary small as H tends to zero and every two adjacent subproblems only have a small overlapping. The layer m in Step 2* is relevant to coarse mesh H (see Lemma 4.2* for detail). And the final finite element solutions in both forms are globally continuous.

4 Theoretical Results

In this section, we will give the theoretical results for Algorithm 1 and Algorithm 2. Firstly, we give the error estimates of Algorithm 1.

By the idea of fictitious domain method (see [10]), we extend the local sub-problem (3.2) to Ω. Let us denote $\Gamma = \partial\Omega$ and $\Gamma_i = \partial\omega_i^1 \backslash \Gamma$. Then, there exists $\xi^i \in H^{-\frac{1}{2}}(\Gamma_i)$ such that the zero extension of $w_{H,h}^i$ satisfies

$$\begin{cases} a(w_{H,h}^i, v) = (f, \phi_i v) - a(u_H, \phi_i v) - \displaystyle\int_{\Gamma_i} \xi^i v \mathrm{d}s, & \forall v \in S_0^h(\Omega), \\ \displaystyle\int_{\Gamma_i} \mu w_{H,h}^i \mathrm{d}s = 0, & \forall \mu \in H^{-\frac{1}{2}}(\Gamma_i). \end{cases} \tag{4.1}$$

Denote

$$\hat{w} = u - u_H \in H_0^1(\Omega),$$

then the residual equation is

$$a(\hat{w}, v) = (f, v) - a(u_H, v), \quad \forall v \in H_0^1(\Omega). \tag{4.2}$$

For the previously defined fine mesh $T^h(\Omega)$ and the associated finite element space $S_0^h(\Omega)$, the Galerkin approximation for (4.2) reads: Find $\hat{w}_H \in S_0^h(\Omega)$ such that

$$a(\hat{w}_H, v) = (f, v) - a(u_H, v), \quad \forall v \in S_0^h(\Omega). \tag{4.3}$$

By the superposition principle, (4.3) can be rewritten as follows: Find $\hat{w}_H^i \in S_0^h(\Omega)$, $i = 1, 2, \cdots, N$, such that

$$a(\hat{w}_H^i, v) = (f, \phi_i v) - a(u_H, \phi_i v), \quad \forall v \in S_0^h(\Omega), i = 1, 2, \cdots, N. \tag{4.4}$$

It is obvious that $\hat{w}_H = \sum\limits_{i=1}^{N} \hat{w}_H^i$.

If we set the local error and the global error of $u_{H,h}$ by

$$e_{H,h}^i = \hat{w}_H^i - w_{H,h}^i, \quad e_{H,h} = \sum_{i=1}^{N} e_{H,h}^i,$$

respectively, it is easy to obtain the following equations

$$a(e_{H,h}^i, v) + \int_{\Gamma_i} \xi^i v \mathrm{d}s = 0, \quad \forall v \in S_0^h(\Omega), i = 1, 2, \cdots, N,$$

and

$$a(e_{H,h}, v) + \sum_{i=1}^{N} \int_{\Gamma_i} \xi^i v \mathrm{d}s = 0, \quad \forall v \in S_0^h(\Omega).$$

For all points $x \in \Omega$, it is clear that there exists a positive integer κ, which has nothing to do with N and x, such that each x belongs to κ different ω_i^1 at most. The following lemma can be found in [15].

Lemma 4.1 The multiplier ξ^i in (4.1) satisfies

$$\|\xi^i\|_{H^{-\frac{1}{2}}(\Gamma_i)} \lesssim \|\nabla e_{H,h}^i\|_{0,\Omega},$$

and

$$\sum_{i=1}^{N} \int_{\Gamma_i} \xi^i v \mathrm{d}s \lesssim \kappa^{\frac{1}{2}} \Big(\sum_{i=1}^{N} \|\xi^i\|_{H^{-\frac{1}{2}}(\Gamma_i)} \Big)^{\frac{1}{2}} \|v\|_{1,\Omega}.$$

Noting that

$$\|\nabla e^i_{H,h}\|^2_{0,\Omega} = \|\nabla(\hat{w}^i_H - w^i_{H,h})\|^2_{0,\Omega} = \|\nabla \hat{w}^i_H\|^2_{0,\Omega\setminus\omega^1_i} + \|\nabla(\hat{w}^i_H - w^i_{H,h})\|^2_{0,\omega^1_i}.$$

For the local error $e^i_{H,h}|_{\omega^1_i}$, it is obvious that

$$a(e^i_{H,h}|_{\omega^1_i}, v) = 0, \quad v \in S^h_0(\omega^1_i), \quad e^i_{H,h}|_{\partial\omega^1_i} = \hat{w}^i_H|_{\partial\omega^1_i}.$$

As $\hat{w}^i_H \in S^h_0(\Omega)$, there holds

$$\|e^i_{H,h}\|_{1,\omega^1_i} \lesssim \|\hat{w}^i_H\|_{\frac{1}{2},\partial\omega^1_i} = \|\hat{w}^i_H\|_{\frac{1}{2},\partial(\Omega\setminus\omega^1_i)} \lesssim \|\nabla \hat{w}^i_H\|_{0,\Omega\setminus\omega^1_i}.$$

Thus, we obtain

$$\|\nabla e^i_{H,h}\|_{0,\Omega} \lesssim \|\nabla \hat{w}^i_H\|_{0,\Omega\setminus\omega^1_i}. \tag{4.5}$$

By (4.5), we give the estimate of $\|\nabla e^i_{H,h}\|_{0,\Omega}$, which plays a crucial role in the following section.

Lemma 4.2 Let us set

$$\alpha_d = \begin{cases} \dfrac{c}{|\ln H|^2}, & d = 2, \\ \dfrac{c}{|\ln H|}, & d = 3, \end{cases}$$

where $c > 0$ is a positive constant that does not depend on H, h, ω^1_i. Then, there holds

$$\|\nabla e^i_{H,h}\|_{0,\Omega} \lesssim H^{\alpha_d}\|\nabla \hat{w}^i_H\|_{0,\Omega}.$$

Proof Let us denote

$$\tilde{\Omega}^0_i = \Omega^0_i = \Omega \setminus \omega^1_i.$$

We extend the domain $\tilde{\Omega}^0_i$ along the outward normal direction on $\partial\tilde{\Omega}^0_i \setminus \partial\Omega$ within Ω by a fine mesh layer to get $\tilde{\Omega}^1_i \supset \tilde{\Omega}^0_i$ and denote by Ω^1_i the incremental annular zone, that is $\Omega^1_i = \tilde{\Omega}^1_i \setminus \tilde{\Omega}^0_i$. Repeat the above procedure until we obtain $\Omega^M_i = \Omega \setminus D_i$, where $M \approxeq \frac{H}{h}$. Then, we get a series of subdomains

$$\tilde{\Omega}^0_i \subset\subset \tilde{\Omega}^1_i \subset\subset \cdots \subset\subset \tilde{\Omega}^M_i,$$

and a series of disjoint annular zones

$$\Omega^0_i, \Omega^1_i, \cdots, \Omega^M_i.$$

It is obvious that

$$\tilde{\Omega}^k_i = \bigcup_{j=0}^{k} \Omega^j_i, \quad k = 0, 1, 2, \cdots, M.$$

Let us define

$$\partial\tilde{\Omega}^k_i = \gamma^k_i \cup \Gamma^k_i,\ \gamma^k_i = \partial\tilde{\Omega}^k_i \setminus \partial\Omega,\ \Gamma^k_i = \partial\tilde{\Omega}^k_i \setminus \gamma^k_i,\ k = 0, 1, 2, \cdots, M.$$

Noting that

$$a(\hat{w}^i_H, v)_{\tilde{\Omega}^k_i} = 0, \quad \forall v \in S^h_0(\tilde{\Omega}^k_i), k = 1, 2, \cdots, M,$$

and $\tilde{\Omega}^k_i = \tilde{\Omega}^{k-1}_i \cup \Omega^k_i$, we derive

$$a(\hat{w}^i_H, v)_{\tilde{\Omega}^{k-1}_i} = -a(\hat{w}^i_H, v)_{\Omega^k_i}, \quad \forall v \in S^h_0(\tilde{\Omega}^k_i). \tag{4.6}$$

Here, we introduce a smooth function $\psi \in S_0^h(\tilde{\Omega}_i^k)$ such that $\psi|_{\gamma_i^k} = 0$ for $k \geq 1$ and

$$\text{supp}\psi = \tilde{\Omega}_i^k, \quad \psi(x) \equiv 1 \, \forall x \in \tilde{\Omega}_i^{k-1}, \quad 0 < \psi < 1 \, \text{and} \, |\nabla\psi(x)| \lesssim h^{-1}.$$

By taking $v = I_h(\psi\hat{w}_H^i) \in S_0^h(\tilde{\Omega}_i^k)$ in (4.6), we have

$$\begin{aligned}\beta^*\|\nabla\hat{w}_H^i\|_{1,\tilde{\Omega}_i^{k-1}}^2 &\leq a(\hat{w}_H^i, \hat{w}_H^i)_{\tilde{\Omega}_i^{k-1}} = -a(\hat{w}_H^i, I_h(\psi\hat{w}_H^i))_{\Omega_i^k} \\ &\leq \|\nabla\hat{w}_H^i\|_{0,\Omega_i^k}\|\nabla I_h(\psi\hat{w}_H^i)\|_{0,\Omega_i^k} \\ &\lesssim \|\nabla\hat{w}_H^i\|_{0,\Omega_i^k}\|\nabla(\psi\hat{w}_H^i)\|_{0,\Omega_i^k}. \end{aligned} \tag{4.7}$$

For $\|\nabla(\psi\hat{w}_H^i)\|_{0,\Omega_i^k}$, we have

$$\|\nabla(\psi\hat{w}_H^i)\|_{0,\Omega_i^k} \leq \|\psi\nabla\hat{w}_H^i\|_{0,\Omega_i^k} + \|\hat{w}_H^i\nabla\psi\|_{0,\Omega_i^k} \leq \|\nabla\hat{w}_H^i\|_{0,\Omega_i^k} + h^{-1}\|\hat{w}_H^i\|_{0,\Omega_i^k}. \tag{4.8}$$

Because of the estimation of $\|\hat{w}_H^i\|_{0,\Omega_i^k}$ in [15], there holds

$$\|\hat{w}_H^i\|_{0,\Omega_i^k}^2 \lesssim hH^{d-1}\beta_d(H)\|\nabla\hat{w}_H^i\|_{0,\tilde{\Omega}_i^k}^2,$$

where $\beta_d(H) = H^{-1}$ when $d = 3$ and $\beta_d(H) = |\ln H|$ when $d = 2$.

As $\|\nabla\hat{w}_H^i\|_{0,\tilde{\Omega}_i^k} \leq \|\nabla\hat{w}_H^i\|_{0,\Omega_i^k} + \|\nabla\hat{w}_H^i\|_{0,\tilde{\Omega}_i^{k-1}}$ and $h^{-\frac{1}{2}}H^{\frac{d-1}{2}}\beta_d^{\frac{1}{2}}(H) > 1$, combining the above estimate with (4.7) and (4.8) admits

$$\begin{aligned}\|\nabla\hat{w}_H^i\|_{0,\tilde{\Omega}_i^{k-1}}^2 &\lesssim \|\nabla\hat{w}_H^i\|_{0,\Omega_i^k}(\|\nabla\hat{w}_H^i\|_{0,\Omega_i^k} + h^{-\frac{1}{2}}H^{\frac{d-1}{2}}\beta_d^{\frac{1}{2}}(H)\|\nabla\hat{w}_H^i\|_{0,\tilde{\Omega}_j^k}) \\ &\leq \|\nabla\hat{w}_H^i\|_{0,\Omega_i^k}^2 + h^{-\frac{1}{2}}H^{\frac{d-1}{2}}\beta_d^{\frac{1}{2}}(H)\|\nabla\hat{w}_H^i\|_{0,\Omega_i^k}(\|\nabla\hat{w}_H^i\|_{0,\Omega_i^k} + \|\nabla\hat{w}_H^i\|_{0,\tilde{\Omega}_i^{k-1}}) \\ &\lesssim h^{-\frac{1}{2}}H^{\frac{d-1}{2}}\beta_d^{\frac{1}{2}}(H)\|\nabla\hat{w}_H^i\|_{0,\Omega_i^k}^2 + h^{-\frac{1}{2}}H^{\frac{d-1}{2}}\beta_d^{\frac{1}{2}}(H)\|\nabla\hat{w}_H^i\|_{\Omega_i^k}\|\nabla\hat{w}_H^i\|_{0,\tilde{\Omega}_i^{k-1}}. \end{aligned}$$

By Young's inequality, we get

$$\|\nabla\hat{w}_H^i\|_{0,\tilde{\Omega}_i^{k-1}}^2 \lesssim h^{-1}H^{d-1}\beta_d(H)\|\nabla\hat{w}_H^i\|_{0,\Omega_i^k}^2,$$

or

$$\|\nabla\hat{w}_H^i\|_{0,\tilde{\Omega}_i^k}^2 \geq chH^{1-d}\beta_d^{-1}(H)\|\nabla\hat{w}_H^i\|_{0,\tilde{\Omega}_i^{k-1}}^2,$$

where $c > 0$ is a constant that does not depend on H, h, i, and k.

By repeating the last inequality, we have

$$\begin{aligned}\|\nabla\hat{w}_H^i\|_{0,\tilde{\Omega}_i^M}^2 &= \|\nabla\hat{w}_H^i\|_{0,\tilde{\Omega}_i^{M-1}}^2 + \|\nabla\hat{w}_H^i\|_{0,\Omega_i^M}^2 \geq (1 + chH^{1-d}\beta_d^{-1}(H))\|\nabla\hat{w}_H^i\|_{0,\tilde{\Omega}_i^{M-1}}^2 \\ &\geq \cdots \geq (1 + chH^{1-d}\beta_d^{-1}(H))^M\|\nabla\hat{w}_H^i\|_{0,\tilde{\Omega}_i^0}^2. \end{aligned}$$

Therefore,

$$\|\nabla\hat{w}_H^i\|_{0,\tilde{\Omega}_i^0}^2 \leq (1 + chH^{1-d}\beta_d^{-1}(H))^{-M}\|\nabla\hat{w}_H^i\|_{0,\tilde{\Omega}_i^M}^2.$$

Being aware of $M \approxeq \frac{H}{h}$ and $\|\nabla\hat{w}_H^i\|_{0,\tilde{\Omega}_j^M} \leq \|\nabla\hat{w}_H^i\|_{0,\Omega}$, simple calculation shows that

$$(1 + chH^{1-d}\beta_d^{-1}(H))^{-M} \approxeq H^{2\alpha_d}.$$

This, together with (4.5), concludes the proof of Lemma 4.2. □

Following the result in Lemma 4.2, we have to give some estimates of $\hat{w}_H^i$ to estimate $\|\nabla e_{H,h}^i\|_{0,\Omega}$.

Lemma 4.3 Suppose that the assumptions A1–A3 are valid. Then, for $i = 1, 2, \cdots, N$, we have

$$\|\nabla\hat{w}_H^i\|_{0,\Omega} \lesssim \|\nabla(u - u_H)\|_{0,D_i}.$$

Proof Using coercive property and taking $v = \hat{w}_H^i$ in (2.5), we can obtain

$$\begin{aligned}\beta^*\|\nabla\hat{w}_H^i\|_{0,\Omega}^2 &\le a(\hat{w}_H^i,\hat{w}_H^i) = (f,\phi_i\hat{w}_H^i) - a(u_H,\phi_i\hat{w}_H^i)\\ &= a(u-u_H,\phi_i\hat{w}_H^i) = a(u-u_H,\hat{I}_H(\phi_i\hat{w}_H^i))\\ &= a(u-u_H,\hat{I}_H(\phi_i I_H\hat{w}_H^i) + \hat{I}_H[\phi_i\hat{I}_H\hat{w}_H^i]),\end{aligned}$$

where $\hat{I}_H = I - I_H$.

Using the continuity property of the bilinear form $a(\cdot,\cdot)$, we have

$$\begin{aligned}&a(u-u_H,\hat{I}_H(\phi_i I_H\hat{w}_H^i) + \hat{I}_H[\phi_i\hat{I}_H\hat{w}_H^i])\\ &\lesssim \|\nabla(u-u_H)\|_{0,D_i}(\|\nabla[\hat{I}_H(\phi_i I_H\hat{w}_H^i)]\|_{0,D_i} + \|\nabla\hat{I}_H[\phi_i\hat{I}_H\hat{w}_H^i]\|_{0,D_i}).\end{aligned}$$

Assume that A1–A2 hold and notice that ϕ_i is a linear function on each τ_Ω^H and $|D\phi_i| \lesssim H^{-1}$, then we can obtain

$$\begin{aligned}\|\nabla[\hat{I}_H(\phi_i I_H\hat{w}_H^i)]\|_{0,D_i} &= (\sum_{\tau_\Omega^H\subset D_i}\|\nabla\hat{I}_H(\phi_i I_H\hat{w}_H^i)\|_{0,\tau_\Omega^H}^2)^{\frac{1}{2}}\\ &\le H(\sum_{\tau_\Omega^H\subset D_i}\|D^2(\phi_i I_H\hat{w}_H^i)\|_{0,\tau_\Omega^H}^2)^{\frac{1}{2}}\\ &\lesssim H(\sum_{\tau_\Omega^H\subset D_i}[\|\phi_i D^2(I_H\hat{w}_H^i)\|_{0,\tau_\Omega^H}^2 + \|D\phi_i D(I_H\hat{w}_H^i)\|_{0,\tau_\Omega^H}^2])^{\frac{1}{2}}\\ &\lesssim H(\sum_{\tau_\Omega^H\subset D_i}[H^{-2}\|D(I_H\hat{w}_H^i)\|_{0,\tau_\Omega^H}^2 + H^{-2}\|D(I_H\hat{w}_H^i)\|_{0,\tau_\Omega^H}^2])^{\frac{1}{2}}\\ &\lesssim \|\nabla\hat{w}_H^i\|_{D_i},\\ \|\nabla\hat{I}_H[\phi_i\hat{I}_H\hat{w}_H^i]\|_{0,D_i} &\lesssim \|D(\phi_i\hat{I}_H\hat{w}_H^i)\|_{0,D_i}\\ &\lesssim \|D\phi_i\hat{I}_H\hat{w}_H^i\|_{0,D_i} + \|\phi_i D(\hat{I}_H\hat{w}_H^i)\|_{0,D_i} \lesssim \|\nabla\hat{w}_H^i\|_{0,D_i}.\end{aligned}$$

Adding the above two equations leads to

$$\|\nabla\hat{w}_H^i\|_{0,\Omega} \lesssim \|\nabla(u-u_H)\|_{0,D_i}.$$

□

Now, we give the error estimations of Algorithm 1 in the following theorem.

Theorem 4.4 Assume that assumptions A1, A2, A3, and (2.7) hold and $u \in H^{r+1}(\Omega)$. Then,

$$\|\nabla(u-u_H^h)\|_{0,\Omega} \lesssim h^r + H^{\alpha_d}\|\nabla(u-u_H)\|_{0,\Omega},$$

$$\|u-u_H^h\|_{0,\Omega} \lesssim h^{r+1} + H\|\nabla(u-u_H^h)\|_{0,\Omega},$$

where $\alpha_d > 0$ is defined in Lemma 4.2.

Proof At the beginning, we introduce an H^1-orthogonal projection P_H from $H_0^1(\Omega)$ onto $S_0^H(\Omega)$: for given $w \in H_0^1(\Omega)$, find $P_H w \in S_0^H(\Omega)$ such that

$$a(v, w - P_H w) = 0, \quad \forall v \in S_0^H(\Omega).$$

It is classical that

$$\|(I-P_H)w\|_\Omega \lesssim H\|\nabla w\|_\Omega, \quad \forall w \in H_0^1(\Omega).$$

Being aware of the definition of $w_{H,h}$ and $\sum_{i=1}^{N}\phi_i = 1$ in Ω, the summation of all the equations of (4.1) gives the equation satisfied by $w_{H,h}$

$$a(w_{H,h}, v) = (f, v) - a(u_H, v) - \sum_{j=1}^{N}\int_{\Gamma_i}\xi^i v\mathrm{d}s, \quad \forall v \in S_0^h(\Omega). \tag{4.9}$$

Hence,

$$a(u_{H,h}, v) = (f, v) - \sum_{i=1}^{N}\int_{\Gamma_i}\xi^i v\mathrm{d}s, \quad \forall v \in S_0^h(\Omega).$$

On the other hand, the coarse mesh correction can be rewritten as

$$a(E_H, v) = (f, P_H v) - a(u_{H,h}, P_H v), \quad \forall v \in S_0^h(\Omega).$$

Combination of the above estimates yields

$$a(u_H^h, v) = (f, v) + (f, P_H v) - a(u_{H,h}, P_H v) - \sum_{i=1}^{N}\int_{\Gamma_i}\xi^i v\mathrm{d}s, \quad \forall v \in S_0^h(\Omega).$$

Finally, we have

$$a(u_H^h, v) = (f, v) - \sum_{j=i}^{N}\int_{\Gamma_i}\xi^i (I - P_H)v\mathrm{d}s, \quad \forall v \in S_0^h(\Omega),$$

and

$$a(u_h - u_H^h, v) = \sum_{i=1}^{N}\int_{\Gamma_i}\xi^i (I - P_H)v\mathrm{d}s, \quad \forall v \in S_0^h(\Omega). \tag{4.10}$$

Using the above error equation of $u_h - u_H^h$, and by Lemmas 4.1–4.3, we obtain

$$\|\nabla(u_h - u_H^h)\|_{0,\Omega} \lesssim H^{\alpha_d}\|\nabla(u - u_H)\|_{0,\Omega}.$$

Because of the triangle inequality, we can easily derive the first result.

The Aubin-Nitsche duality argument is necessary for the L^2-error estimate. Suppose that A3 is valid, then for $u_h - u_H^h \in L^2(\Omega)$, there exists $\phi \in H^2(\Omega) \cap H_0^1(\Omega)$ such that

$$a(v, \phi) = (u_h - u_H^h, v), \quad \forall v \in H_0^1(\Omega),$$

and

$$\|\phi\|_{2,\Omega} \lesssim \|u_h - u_H^h\|_{0,\Omega}.$$

Taking $v = u_h - u_H^h$ and noting (4.10), we have

$$\|u_h - u_H^h\|_{0,\Omega}^2 \le a(u_h - u_H^h, \phi) = a(u_h - u_H^h, (I - P_H)\phi).$$

Consequently,

$$\begin{aligned}\|u_h - u_H^h\|_{0,\Omega}^2 &\le a(u_h - u_H^h, (I - P_H)\phi) \lesssim \|\nabla(u_h - u_H^h)\|_{0,\Omega}\|\nabla(I - P_H)\phi\|_{0,\Omega} \\ &\lesssim H\|\nabla(u_h - u_H^h)\|_{0,\Omega}\|\phi\|_{2,\Omega} \lesssim H\|\nabla(u_h - u_H^h)\|_{0,\Omega}\|u_h - u_H^h\|_{0,\Omega}.\end{aligned}$$

By combining triangle inequality, we finish the L^2-error estimate. □

It is well known that if $u \in H_0^1(\Omega) \cap H^{r+1}(\Omega)$ and u_{TG} is the two-grid finite element approximation, there holds

$$\|u - u_{TG}\|_{1,\Omega} \lesssim h^r + H^{r+1},$$

$$\|u - u_{TG}\|_{0,\Omega} \lesssim h^{r+1} + H^{r+2}.$$

As our algorithms could be seen as varied two-grid methods, therefore, we expect our methods can reach the same convergence order with the two-grid method, which we called optimal error.

From the above results, it is easy to observe that we can improve the convergence order of both H^1 and L^2 errors of the coarse mesh standard Galerkin approximation u_H for α_d order by one two-grid iteration, and this phenomenon suggests us to do the following two-grid iteration with

$$K = [\alpha_d^{-1} + 0.5].$$

- (Step 0) Let $k = 0$ and solve (3.1) to obtain $u_H \in S_0^H(\Omega)$, and we set $u_H^{0,h} = u_H$;
- (Step 1) Solve the equations in (3.2) with $u_H = u_H^{k,h}$ to get $\{w_{H,h}^i\}_{i=1}^N$, which are denoted by $\{w_{H,h}^{k+1,i}\}_{i=1}^N$. Then, we derive $u_{H,h}^{k+1}$ by (3.3);
- (Step 2) Solve (3.4) with $u_{H,h} = u_{H,h}^{k+1}$ to get E_H^{k+1} and define

$$u_H^{k+1,h} = u_{H,h}^{k+1} + E_H^{k+1};$$

if $k+1 > K$, stop the iteration and denote $u_H^h = u_H^{k+1,h}$, which is the final approximation with optimal error. Otherwise, let $k := k+1$ and goto (Step 1).

Corollary Assume $u \in H_0^1(\Omega) \cap H^{r+1}(\Omega)$, the final approximation u_H^h of scheme (Step 0)–(Step 2) has the following error estimates

$$\|u - u_H^h\|_{1,\Omega} \lesssim h^r + H^{r+1}, \tag{4.11}$$

$$\|u - u_H^h\|_{0,\Omega} \lesssim h^{r+1} + H^{r+2}. \tag{4.12}$$

Next, we give the the error estimations of Algorithm 2 in the same way.

Without distinction, we still use the same notions $\Gamma = \partial\Omega$ and $\Gamma_i = \partial\omega_i \backslash \Gamma$, and

$$\hat{e}_{H,h}^i = \hat{w}_H^i - \hat{w}_{H,h}^i, \quad \hat{e}_{H,h} = \sum_{i=1}^N \hat{e}_{H,h}^i,$$

the local error and the global error of $u_{H,h}$, respectively.

It is obvious that Lemma 4.1 and Lemma 4.3 remain the same forms, while for Lemma 4.2, we do a little modification and get the following lemma.

Lemma 4.2* For a proper chosen m,

$$m = \begin{cases} \dfrac{|\ln H|^2}{c}, & d = 2, \\ \dfrac{|\ln H|}{c}, & d = 3, \end{cases}$$

where $c > 0$ is a positive constant that does not depend on H, h, ω_i. We have

$$\|\nabla \hat{e}_{H,h}^i\|_{0,\Omega} \lesssim H \|\nabla \hat{w}_H^i\|_{0,\Omega}.$$

Proof In the same way, we have

$$\|\nabla \hat{w}_H^i\|_{0,\tilde{\Omega}_i^0}^2 \leq (1 + chH^{1-d}\beta_d^{-1}(H))^{-M} \|\nabla \hat{w}_H^i\|_{0,\tilde{\Omega}_i^M}^2.$$

Noting $M \approxeq \frac{mH}{h}$ and $\|\nabla \hat{w}_H^i\|_{0,\tilde{\Omega}_j^M} \leq \|\nabla \hat{w}_H^i\|_{0,\Omega}$, simple calculation shows that

$$(1 + chH^{1-d}\beta_d^{-1}(H))^{-M} \approxeq H^2.$$

This, together with (4.5), concludes the proof of the lemma. □

Theorem 4.5 Assume that assumptions A1, A2, A3, and (2.7) hold and $u \in H^{r+1}(\Omega)$. Then

$$\|\nabla(u - \hat{u}_H^h)\|_{0,\Omega} \lesssim h^r + H\|\nabla(u - u_H)\|_{0,\Omega},$$
$$\|u - \hat{u}_H^h\|_{0,\Omega} \lesssim h^{r+1} + H\|\nabla(u - \hat{u}_H^h)\|_{0,\Omega}.$$

5 Numerical Experiments

In this section, we will report some numerical examples (2D and 3D) to complement the analysis results. In the 2D experiments, the domain Ω is the unit square $\Omega = (0,1) \times (0,1)$ with a uniform triangulation $T^H(\Omega) = \{\tau_\Omega^H\}$. In the 3D experiments, the domain Ω is the unit cube $\Omega = (0,1)^3$ with a uniform triangulation $T^H(\Omega) = \{\tau_\Omega^H\}$. P_1 element is employed for the finite element discretization. And all the following numerical results are obtained by using the public domain software FreeFem++.

5.1 2D-Example

For both Algorithm 1 and Algorithm 2, to reach the H^1 accuracy, we should choose H and h such that $h \sim H^2$. With such configuration, we have

$$\|u - u_H^h\|_{1,\Omega} \lesssim H^2, \quad \|u - \hat{u}_H^h\|_{1,\Omega} \lesssim H^2. \tag{5.1}$$

On the other hand, to reach the L^2 accuracy, we should choose H and h such that $h^2 \sim H^3$. In this case,

$$\|u - u_H^h\|_{0,\Omega} \lesssim H^3, \quad \|u - \hat{u}_H^h\|_{0,\Omega} \lesssim H^3. \tag{5.2}$$

In the first experiment, we take $\mathbf{b} = (1.0, 1.0)^T$ and consider the problem with the following analytic solution

$$u(x,y) = 100(x^2 - 2x^3 + x^4)(y - 3y^2 + 2y^3).$$

Then, we can get $f(x,y)$ in (2.1).

In the following Table 1 and Table 2, we give some numerical results according to the above configurations of H and h. For numerical experiments that the true solution u is known, we define the convergence order "ORDER_1" with respect to the coarse mesh size H as

$$\mathrm{ORDER}_1(u_{app}) = \begin{cases} 1 + \dfrac{\ln \frac{\|\nabla(u-u_H)\|_{0,\Omega}}{\|\nabla(u-u_{app})\|_{0,\Omega}}}{|\ln H|}, & H^1 \text{ error order}, \\ 2 + \dfrac{\ln \frac{\|u-u_H\|_{0,\Omega}}{\|u-u_{app}\|_{0,\Omega}}}{|\ln H|}, & L^2 \text{ error order}. \end{cases}$$

The symbol u_{app} stands for certain approximation of u defined in the algorithms. "Iteration" stands for the number of iterations that are used for deriving the final approximation in Algorithm 1, and "m" stands for the patch of layer m that is necessary to obtain optimal error in Algorithm 2.

As seen from Table 1 and Table 2, both Algorithm 1 and Algorithm 2 reach almost the same accuracy as the fine mesh standard Galerkin approximation in H^1-norm and L^2-normal. For H^1-normal, 2 iterations are sufficient for Algorithm 1 and 2 patches of layer for Algorithm 2. Compared with the fine mesh standard Galerkin method, our algorithms can get better accuracy in L^2-normal.

Table 1 H^1**-Error** $(h = H^2)$

$\frac{1}{H}$	8	16	24
$\|\nabla(u-u_H)\|_{0,\Omega}$	$6.8371e-1$	$3.4949e-1$	$2.3397e-1$
$\|\nabla(u-u_h)\|_{0,\Omega}$	$8.7995e-2$	$2.2009e-2$	$9.7818e-3$
$\|\nabla(u-u_H^h)\|_{0,\Omega}$	$8.8021e-2$	$2.2015e-2$	$9.7888e-3$
$\mathrm{ORDER}_1(u_H^h)$	1.99	2.00	2.00
Iteration	2	2	2
$\|\nabla(u-\hat{u}_H^h)\|_{0,\Omega}$	$9.0382e-2$	$2.2918e-2$	$1.0332e-2$
$\mathrm{ORDER}_1(\hat{u}_H^h)$	1.97	1.98	1.98
m	2	2	2

Table 2 L^2**-Error** $(h = H^{\frac{3}{2}})$

$\frac{1}{H}$	25	36	49
$\|u-u_H\|_{0,\Omega}$	$3.3784e-3$	$1.6347e-3$	$8.8361e-4$
$\|u-u_h\|_{0,\Omega}$	$1.3597e-4$	$4.5545e-5$	$1.8145e-5$
$\|u-u_H^h\|_{0,\Omega}$	$1.1502e-4$	$3.8161e-5$	$1.8177e-5$
$\mathrm{ORDER}_1(u_H^h)$	3.05	3.05	3.00
Iteration	1	1	2
$\|u-\hat{u}_H^h\|_{0,\Omega}$	$1.1498e-4$	$3.8173e-5$	$1.3358e-5$
$\mathrm{ORDER}_1(\hat{u}_H^h)$	3.05	3.05	3.08
m	1	1	2

In Figure 2, we show the evolution of error in H^1-normal with "Iteration" (patch of layer) for Algorithm 1 (Algorithm 2). It is clear that the error of Algorithm 1 (Algorithm 2) decays rapidly with respect to "Iteration" (patch of layer).

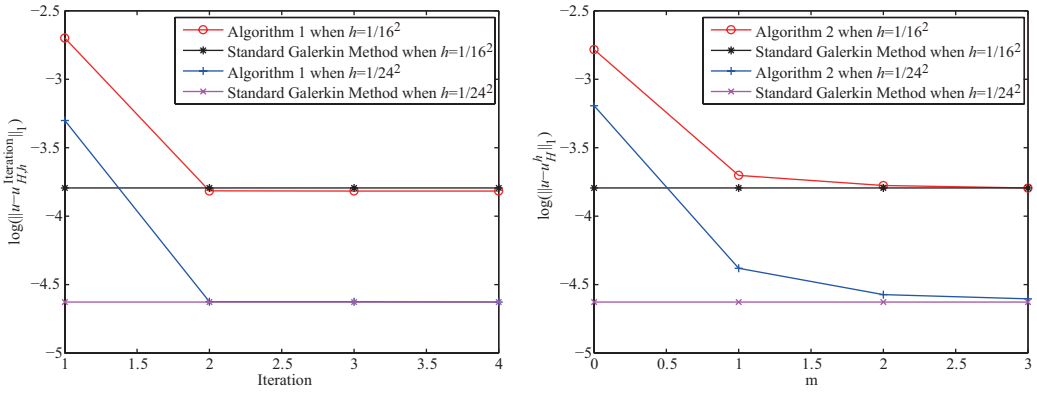

Figure 2 Left: evolution of error in H^1-normal with "Iteration" for Algorithm 1; right: evolution of error in H^1-normal with patch of layer for Algorithm 2

In the second example, we take $\mathbf{b} = (2x - e^y, 3y\cos(\pi x))^T$, and $f = 70\log((x+0.1)(\sin(\pi y)+1))$ in (2.1). As the exact solution u is unknown, the convergence order of the approximate

solution is calculated as

$$\mathrm{ORDER}_2(u_{app}) = \begin{cases} 1 + \dfrac{\ln \frac{\|\nabla(u_h - u_H)\|_{0,\Omega}}{\|\nabla(u_h - u_{app})\|_{0,\Omega}}}{|\ln H|}, & H^1 \text{ error order}, \\ 2 + \dfrac{\ln \frac{\|u_h - u_H\|_{0,\Omega}}{\|u_h - u_{app}\|_{0,\Omega}}}{|\ln H|}, & L^2 \text{ error order}. \end{cases}$$

Here, u_h is the standard Galerkin approximation in the fine mesh finite element space $S_0^h(\Omega)$ and the symbol u_{app} stands for certain approximation of u defined in the proposed algorithms. It is generally known that the H^1 error estimate of the fine mesh standard Galerkin approximation admits the following estimation when $h = H^2$

$$\|\nabla(u - u_h)\|_{0,\Omega} = O(h) = O(H^2),$$

the "$\mathrm{ORDER}_2(u_{app})$" calculated by the above formula equals to 2 means

$$\|\nabla(u_h - u_{app})\|_{0,\Omega} = O(H^2),$$

therefore

$$\|\nabla(u - u_{app})\|_{0,\Omega} = O(H^2).$$

Similarity,

$$\|u - u_{app}\|_{0,\Omega} = O(H^3).$$

The Table 3 and Table 4 report the numerical results of this test problem. It is clear that the errors obtained by the two algorithm are almost identical with each other and confirm the theoretical results.

Table 3 H^1**-Error** ($h = H^2$)

$\frac{1}{H}$	8	16	24
$\|\nabla(u_h - u_H)\|_{0,\Omega}$	$1.8407e-0$	$9.7354e-1$	$6.5736e-1$
$\|\nabla(u_h - u_H^h)\|_{0,\Omega}$	$9.4763e-2$	$4.1015-2$	$2.5572e-2$
$\mathrm{ORDER}_2(u_H^h)$	2.43	2.14	2.02
Iteration	1	1	1
$\|\nabla(u_h - \hat{u}_H^h)\|_{0,\Omega}$	$9.4723e-2$	$4.1003-2$	$2.5574e-2$
$\mathrm{ORDER}_2(\hat{u}_H^h)$	2.43	2.14	2.02
m	1	1	1

Table 4 L^2**-Error** ($h = H^{\frac{3}{2}}$)

$\frac{1}{H}$	25	36	49
$\|u_h - u_H\|_{0,\Omega}$	$8.1035e-3$	$3.9795e-3$	$2.1721e-3$
$\|u_h - u_H^h\|_{0,\Omega}$	$2.6319e-4$	$5.6307e-5$	$3.0138e-5$
$\mathrm{ORDER}_2(u_H^h)$	3.06	3.19	3.10
Iteration	1	2	2
$\|u_h - \hat{u}_H^h\|_{0,\Omega}$	$2.6319e-4$	$6.0148e-5$	$3.2027e-5$
$\mathrm{ORDER}_2(\hat{u}_H^h)$	3.06	3.17	3.08
m	1	2	2

5.2 3D-example

In this section, we will give two 3D examples. In these two examples, the domain Ω is the unit cube $(0,1)^3$ and $\mathbf{b}=(1,1,1)$. In the first 3-D example, we consider the test problem with the the following analytic solution

$$u(x,y,z)=100(x^2-2x^3+x^4)(y-3y^2+2y^3)(z^3-z).$$

The numerical results are given in Tables 5 and 6.

Table 5 H^1**-Error** $(h=H^2)$

$\frac{1}{H}$	6	8	10
$\|\nabla(u-u_H)\|_{0,\Omega}$	$2.9515e-1$	$2.2774e-1$	$1.8467e-1$
$\|\nabla(u-u_h)\|_{0,\Omega}$	$5.9048e-2$	$3.3496e-2$	$2.1515e-2$
$\|\nabla(u-u_H^h)\|_{0,\Omega}$	$5.9194e-2$	$3.3599e-2$	$2.1696e-2$
$\mathrm{ORDER}_1(u_H^h)$	1.89	1.92	1.93
Iteration	2	2	2
$\|\nabla(u-\hat{u}_H^h)\|_{0,\Omega}$	$6.0408e-2$	$3.5356e-2$	$2.2719e-2$
$\mathrm{ORDER}_1(\hat{u}_H^h)$	1.89	1.90	1.91
m	2	2	2

Table 6 L^2**-Error** $(h=H^{\frac{3}{2}})$

$\frac{1}{H}$	9	16	25
$\|u-u_H\|_{0,\Omega}$	$8.6338e-3$	$2.8568e-3$	$1.1850e-3$
$\|u-u_h\|_{0,\Omega}$	$1.2840e-3$	$2.3929e-4$	$6.3981e-5$
$\|u-u_H^h\|_{0,\Omega}$	$1.3024e-3$	$2.3795e-4$	$6.2568e-5$
$\mathrm{ORDER}_1(u_H^h)$	2.86	2.90	2.91
Iteration	2	2	2
$\|u-\hat{u}_H^h\|_{0,\Omega}$	$1.3338e-3$	$2.4903e-4$	$6.7538e-5$
$\mathrm{ORDER}_1(\hat{u}_H^h)$	2.85	2.88	2.89
m	2	2	2

Table 7 H^1**-Error** $(h=H^2)$

$\frac{1}{H}$	6	8	10
$\|\nabla(u_h-u_H)\|_{0,\Omega}$	3.1859	2.5719	2.1384
$\|\nabla(u_h-u_H^h)\|_{0,\Omega}$	$5.9544e-1$	$4.0252e-2$	$2.9719e-2$
$\mathrm{ORDER}_2(u_H^h)$	1.94	3.00	2.86
Iteration	1	2	2
$\|\nabla(u_h-\hat{u}_H^h)\|_{0,\Omega}$	$6.2390e-1$	$4.2773-2$	$3.0909e-2$
$\mathrm{ORDER}_2(\hat{u}_H^h)$	1.91	2.97	2.84
m	1	2	2

Table 8 L^2**-Error** ($h = H^{\frac{3}{2}}$)

$\frac{1}{H}$	9	16	25
$\|u_h - u_H\|_{0,\Omega}$	$7.7114e-2$	$2.8568e-2$	$1.2454e-2$
$\|u_h - u_H^h\|_{0,\Omega}$	$5.7182e-3$	$1.5811e-3$	$4.2787e-5$
$\mathrm{ORDER}_2(u_H^h)$	3.18	3.04	3.76
Iteration	1	1	2
$\|u_h - \hat{u}_H^h\|_{0,\Omega}$	$6.2994e-3$	$1.6892e-3$	$4.4557e-5$
$\mathrm{ORDER}_2(\hat{u}_H^h)$	3.14	3.02	3.75
m	1	1	2

The second example of 3-D case is a test problem driven by the following free term

$$f = 70\log((x+0.1)(\sin\pi y+1)(z+0.1)(\sin\pi z+1)),$$

$$\mathbf{b} = (2xy - e^z, 3xz\cos\pi y, \sin\pi x\sin\pi y\sin\pi z),$$

whose numerical results are given in Tables 7 and 8.

6 Conclusions

In this article, we have shown and analyzed two expandable two-grid parallel finite element methods for solving the linear elliptic problems. For Algorithm 1, a few iterations, say $O(|\ln H|^2)$ or $O(|\ln H|)$ in 2-D or 3-D respectively, are essential to obtain optimal error; while for Algorithm 2, patches of diameter $O(|\ln H|^2)H$ or $O(|\ln H|)H$ in 2-D or 3-D respectively are sufficient to guarantee to preserve the optimal convergence order. The numerical results and theoretical results keep consistent. Therefore, both the two algorithms can be regarded as flexible methods.

References

[1] Adams R A. Sobolev Spaces. New York: Academic Press, 1975

[2] Appelhans D, Manteuffel T, McCormick S, Ruge J. A low-communication, parallel algorithm for solving PDEs based on range decomposition. Numer Linear Algebra Appl, 2017, **24**: e2041. doi: 10.1002/nla.2041

[3] Babuška I, Melenk J. The partition of unity method. Int J Numer Meth Eng, 1997, **40**: 727–758

[4] Bank R, Jimack P. A new parallel domain decomposition method for the adaptive finite element solution of elliptic partial differential equations. Concurrency Computat: Pract Exper, 2001, **13**: 327–350

[5] Ciarlet P G. The finite element method for elliptic problems. SIAM Classics in Appl Math 40. Philadelphia: SIAM, 2002

[6] Du G, Zuo L. A two-grid parallel partition of unity finite element scheme. Numer Algorithms, 2019, **80**: 429–445

[7] Du G, Hou Y, Zuo L. Local and parallel finite element methods for the mixed Navier-Stokes/Darcy model. Int J Comput Math, 2016, **93**: 1155–1172

[8] Du G, Hou Y, Zuo L. A modified local and parallel finite element method for the mixed Stokes-Darcy model. J Math Anal Appl, 2016, **435**: 1129–1145

[9] Du G, Zuo L. Local and parallel finite element method for the mixed Navier-Stokes/Darcy model with Beavers-Joseph interface conditions. Acta Mathematica Scientia, 2017, **37B**: 1331–1347

[10] Girault V, Glowinski R, López H, Vila J -P. A boundary multiplier/fictitious domain method for the steady incompressible Navier-Stokes equations. Numer Math, 2001, **88**: 75–103

[11] Målqvist A, Peterseim D. Localization of elliptic multiscale problems. Math Comput, 2012, **83**: 2583–2603

[12] He Y, Mei L, Shang Y, Cui J. Newton iterative parallel finite element algorithm for the steady Navier-Stokes equations. J Sci Comput, 2010, **44**: 92–106

[13] He Y, Xu J, Zhou A. Local and parallel finite element algorithms for the Navier-Stokes problem. J Comput Math, 2006, **24**: 227–238

[14] He Y, Xu J, Zhou A, Li J. Local and parallel finite element algorithms for the Stokes problem. Numer Math, 2008, **109**: 415–434

[15] Hou Y, Du G. An Expandable Local and Parallel Two-Grid Finite Element Scheme. Comput Math Appl, 2016, **71**: 2541–2556

[16] Larson M G, Malqvist A. Adaptive Variational Multi-scale Methods Based on a Posteriori Error Estimation: Energy Norm Estimates for Elliptic Problems. Comput Method Appl M, 2007, **196**: 2313–2324

[17] Melenk J, Babuška I. The partition of unity finite element method: basic theory and applications. Comput Method Appl M, 1996, **139**: 289–314

[18] Shang Y, He Y. A parallel Oseen-linearized algorithm for the stationary Navier-Stokes equations. Comput Method Appl M, 2012, **209-212**: 172–183

[19] Song L, Hou Y, Zheng H. Adaptive Local Postprocessing Finite Element Method for the Navier-Stokes Equations. J Sci Comput, 2013, **55**: 255–267

[20] Xu J, Zhou A. Local and parallel finite element algorithms based on two-grid discretizations. Math Comput, 2000, **69**: 881–909

[21] Xu J, Zhou A. Local and Parallel Finite Element Algorithms Based on Two-Grid Discretizations for Nonlinear Problems. Adv Comput Math, 2001, **14**: 293–327

[22] Yu J, Shi F, Zheng H. Local and parallel finite element method based on the partition of unity for the stokes problem. SIAM J Sci Comput, 2014, **36**: C547–C567

[23] Zheng H, Song L, Hou Y, Zhang Y. The partition of unity parallel finite element algorithm. Adv Comput Math, 2014, **41**: 937–951

[24] Zheng H, Yu J, Shi F. Local and parallel finite element method based on the partition of unity for incompressible flow. J Sci Comput, 2015, **65**: 512–532

[25] Zheng H, Shi F, Hou Y, et al. New local and parallel finite element algorithm based on the partition of unity. J Math Anal Appl, 2016, **435**: 1–19